

Article

Optimizing the Shading Device Configuration of Kinetic Façades through Daylighting Performance Assessment

Dong-Hyun Kim , Hieu Trung Luong and Trang Thao Nguyen 

Department of Architecture, Sejong University, Seoul 05005, Republic of Korea; luongtrunghieu.05@gmail.com (H.T.L.); nguyenthaotrang90@gmail.com (T.T.N.)

* Correspondence: dkim@sejong.ac.kr

Abstract: When designing a façade, it is essential to consider the impact of daylight and how it can be optimized through external movable shading devices. To accurately evaluate the lighting performance of a kinetic façade, it is crucial to consider the operation of these shading devices, as they can significantly impact performance. This study proposes a high-precision methodology that utilizes digital tools and hourly data to examine the effectiveness of dynamic shading device systems in enhancing daylight performance and optimizing shading configurations using the Genetic Optimization algorithm. The study's results demonstrate that the proposed methodology is accurate and effective, showing that the optimal operation scenario can exceed LEED v4.1 requirements while meeting daylight availability standards. Designers can achieve optimal performance by adjusting each parameter for a lighting energy-conserving kinetic façade. The limitations and applicability of this method are also discussed.

Keywords: façade design; kinetic façade; lighting performance; movable shading devices; LEED v4.1



Citation: Kim, D.-H.; Luong, H.T.; Nguyen, T.T. Optimizing the Shading Device Configuration of Kinetic Façades through Daylighting Performance Assessment. *Buildings* **2024**, *14*, 1038. <https://doi.org/10.3390/buildings14041038>

Academic Editor: Danny Hin Wa Li

Received: 6 March 2024

Revised: 1 April 2024

Accepted: 4 April 2024

Published: 8 April 2024



Copyright: © 2024 by the authors. Licensee MDPI, Basel, Switzerland. This article is an open access article distributed under the terms and conditions of the Creative Commons Attribution (CC BY) license (<https://creativecommons.org/licenses/by/4.0/>).

1. Introduction

The significance of lighting design in architecture is crucial for achieving energy efficiency and ensuring user comfort. Contemporary architects often integrate large windows to maximize natural light in buildings, which can lead to issues like solar heat gain and glare. Fixed shading devices, commonly used to address these challenges, have limitations in adapting to the changing sun angle and may hinder access to daylight. In contrast, movable shading devices like kinetic façades can dynamically adjust in real-time, significantly improving indoor thermal comfort and creating a healthier light environment.

Kinetic façades fall into two main categories: motion and shape. Zuk and Clack [1] coined the motion category, describing elements with displacement or kinetic movement. Moloney [2] further detailed kinetic movement modes like folding and expanding.

Al-Masrani et al. [3] extensively studied shading devices from 2005 to 2018, categorizing solar shading systems into passive, active, and hybrid types. They highlighted the complexity of motion dynamics, classifying dynamic shading systems into conventional models with simple motions (e.g., venetian blinds) and innovative models with complex motions (e.g., parametric geometries).

Tabadkani et al. [4] conducted a comprehensive study categorizing adaptive façades based on adaptation mechanisms and user interactions. The inquiry identified ten typological approaches, considering contextual factors, climate, and user engagement. Responsive façades emerged as the most versatile, allowing users to enhance performance while reducing energy consumption. The study classified adaptive façades into simple motion (e.g., venetian blinds) and complex motion (e.g., biomimetic façades), exploring unconventional design scenarios like 3D motion, foldable structures, and biological emulation.

In the field of kinetics, two fundamental modes dominate both individual and coordinated movements. The taxonomy of kinetic forms is based on the angular relation between

solar azimuth and the shading panel's normal vector. Among these, responsive façades can be distilled into three archetypal configurations: vertical, horizontal, and multi-directional shading devices, each with unique modes of movement.

Studies on dynamic façades between 2018 and 2023 (Table 1) primarily focused on a specific type of shading panel. Fixed shading devices, particularly egg-crate designs, were extensively studied for their effectiveness in enhancing daylight and thermal performance in tropical regions [3]. However, these devices face challenges with changing weather conditions. Advanced mechanical shading designs have been criticized for their complexity, cost, and high energy consumption. While hybrid systems combining sustainable solutions show promise, further investigation is needed to assess their environmental and energy performances. The practical implementation of shape-morphing systems in tropical areas is limited, posing challenges due to the climate. Essential design factors, including energy engagement, control methods, and model optimization, are crucial for developing effective shading systems.

Table 1. Studies on dynamic shading systems (2018–2023).

Cite No.	Author	Researched Shading Devices
[5]	Jayathissa, P et al., (2018)	Adaptive solar façade
[6]	Hosseini, S. M., Mohammadi, M., & Guerra-Santin, O. (2019)	2D and 3D rectangle transformation module façade SD
[7]	Im et al., (2019)	Oculi kinetic façade system
[8]	Nakapan, W., & Pattanasirimongkol, A. (2019)	Kinetic façade made of vertical aluminum fins
[9]	Yoon, J. (2019)	Kinetic SMP applications in circular cell-type shading devices with five different morphologies
[10]	Hosseini et al., (2020)	Integration of interactive kinetic façade with colored glass
[11]	Karaseva, L. V., & Cherchaga, O. A. (2021)	Mashrabiya-inspired façade module component
[12]	Hosseini, S. M., Fadli, F., & Mohammadi, M. (2021)	Vertical and horizontal louvres
[13]	Kim, J.-H., & Han, S.-H. (2022)	Multilayered and complex kinetic façade form inspired by dense mass and curvature intersected vectors
[14]	Khidmat et al., (2022)	Horizontal louver with rotatable right and left edges
[15]	Chandrasekaran, C., Sasidhar, K., & Madhumathi, A. (2022)	Electrochromic-applied kinetic louvers
[16]	Sankaewthong et al., (2022)	Expanded-metal shading
[17]	Hosseini, S.M., & Heidari, S. (2022)	Fixed and dynamic vertical-folding SD
[18]	Sadegh et al., (2022)	SD module merging physical DNA and phototropism behavior, compared with vertical static louvre and vertical rotating louvre
[19]	Sanakaewthong et al., (2022)	Kinetic façade of hexagonal modular shapes in grid forms
[20]	Sangtarash et al., (2022)	Triangular module and triangular grid SD
[21]	Rafati, N., Hazbei, M., Eicker, U. (2023)	Louwer
[22]	Kahramanoğlu, B., & Çakıcı Alp, N. (2023)	Miura-ori-based responsive façade
[23]	Choi, H. S (2023)	Hexagon cell module components

This research delves into the efficacy of three mechanized shading device types for providing and regulating adequate daylight within an indoor space. Rather than focusing solely on a specific shading device category and pinpointing the most effective parameters for such devices, this study facilitates a comparative assessment of the efficiency among widely used commercial shading devices, aiming to identify the most suitable option. The primary goal is to enhance daylighting adequacy within an Incheon, Korea, office equipped with a kinetic sun shading system. To achieve this, the study employs a parametric optimization approach to determine the most appropriate shading device types, their 'near-optimal' dimensions, and the optimal rotation angles for dynamic shading devices to meet the daylighting requirements outlined in LEED v4.1.

2. Materials and Methods

The simulation technique used in this study is based on Christoph Reinhart's "Daylighting Handbook II" [24] and involves simulating different settings of shading devices

over discrete time intervals using a phase method. This could include adjusting the position, angle, or characteristics of the shading device to control the amount of daylight entering the space. A set of daylight metrics is calculated for each configuration, considering factors like illuminance levels and glare potential. The algorithm selects the optimal shading configuration for each hour based on predefined triggers such as internal illuminance or external irradiance levels. This approach aims to optimize daylighting performance in buildings by identifying the most effective shading configurations while maintaining occupant comfort and energy efficiency.

2.1. Formulating Configuration Parameters

2.1.1. Indoor Space Parameters

The research space, modelled on the DOE Commercial Reference Building [25] was resized to 4 m × 6 m × 4 m and enhanced with a dynamic façade system featuring a south-facing full-height window and movable shading devices. It can be seen in Table 2 that adjustments, such as a 95% glazing high window, were made for practicality and reduced computational workload. Illuminance calculations will focus on a grid-based, superficial rectangular zone with 0.5 m × 0.5 m segments, ensuring precision and computational efficiency. A standard working plane height of 0.7–0.8 m, aligning with desk surfaces, will be used for accurate daylight simulation.

Table 2. Research space parameter.

Internal Surface and Window Parameter	
Walls	Reflectance = 50%
Ceiling	Reflectance = 80%
Floor	Reflectance = 20%
Shading device	Reflectance = Metal diffuses
Glazing	VT = 95%

2.1.2. Formulating Configuration Parameters of the Shading Panel

The primary focus of this study is to evaluate and optimize shading devices based on their impact on daylighting performance. To achieve this goal, it is necessary to consider the relationship between the shading panel's surface and solar radiation and the sun-path script. Three types of shading device shapes were considered: vertical, horizontal, and multi-directional. The simplest shading device configurations in geometry and movement were selected as experimental prototypes to simplify the research process and minimize computational complexity (Table 3).

Parametric models were generated using Rhinoceros 7 and its plugin—Grasshopper software platforms, focusing on the solid's motion and how the shading panel changes its surface angle with the sun's radiation direction.

Table 3. Formulating configuration parameters of the shading panels.

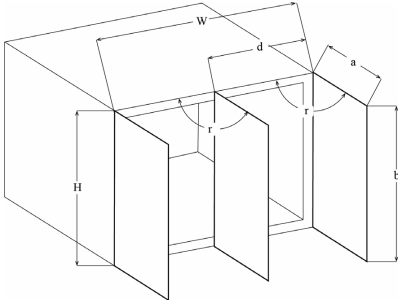
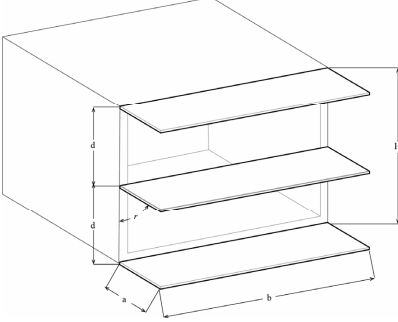
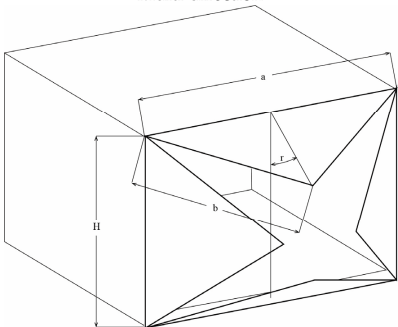
Panel Type	Size	a (m)	b (m)	d (m)	n	r (°)
	Min	0.2			20	0
	Default	W*/n			5	90
	Max	2	4	a	2	180

Table 3. Cont.

Panel Type	Size	a (m)	b (m)	d (m)	n	r (°)
	Horizontal	Min	0.2		20	0
		Default	H^*/n		5	90
	Max	2	4	a	2	180
	Multi-direction	Min	0.2	$\frac{a\sqrt{2}}{10}$	20	0
		Default	H^*/n	$\frac{a\sqrt{2}}{2}$	5	45
	Max	2	4	$2a\sqrt{2}$	1	90

* Note: $H = W = 4$ m.

The parametric models allowed for a better understanding of the operation process of the movable panels. Analysis of the movement of each shading panel in the system revealed that it was possible to maintain the system's movement by rotating the panels along their hinges to open and close the skin, allowing for a closed cycle path of movement from end to end.

Different combinations of shading panel sizes and rotation angles were analyzed, leading to various daylight performances. These two variables, shading panel size and rotation angle, were the primary design parameters controlled using numeric slides. Overall, this approach allowed for a detailed examination of the shading device's impact on daylighting performance while minimizing complexity and computation time.

2.1.3. Daylighting Calculation Parameters

1. Ambient Parameter: For accurate radiance simulation in a low-complexity scene, such as a typical side-lit space with a standard window, use the parameters recommended in Table 4.

Table 4. Selected values of ambient parameters used in this research.

Ambient Bounces (-ab)	Ambient Accuracy (-aa)	Ambient Divisions (-ad)	Ambient Super Samples (-as)	Ambient Resolution (-ar)
4	0.10	1500	1024	100

2. Sun-Path Diagram and Daylight Deflection Scheme: Utilize a sun-path diagram and daylight deflection scheme to establish solar angles and optimal louvre tilt angles at different times of the day and month, especially for specific latitudes. These parameters are crucial for solar shading design, a focus of this study. Solar angle changes for March, June, September, and December in Incheon, South Korea, are sourced from Honeybee.

Assumptions and simulation conditions for feasibility and accuracy:

1. Simulations focus on the 21st day of March, June, September, and December to represent the beginning of each season, providing reliable results for seasonal evaluations.
2. The dynamic façade system under investigation in this research is designed to dynamically respond to environmental changes driven by the movement of the sun. Consequently, the climatic conditions and geographical features of the location play pivotal roles in deriving meaningful findings. Considering this contextual relevance, Incheon, South Korea, was selected as the primary experimental site, thereby facilitating more informed design decisions and practical implementations of dynamic façade technology.
3. Research focuses on basic geometrical shading panels (horizontal, vertical, multi-directional). A fixed distance parameter of 10 cm between shading panels is set for accurate evaluation under given conditions.
4. Configuration parameters include the number of shading devices on a specific façade area and the tilt angle of shading panels. Simulations will cover five different sizes for each shading shape, representing various panel dimensions commonly used in practice. The variable “*n*” denotes the number of shading devices on the façade, with values of 2, 4, 5, 8, and 16, corresponding to panel dimensions of 2 m, 0.8 m, 0.5 m, and 0.25 m.

2.2. Methodology of Optimizing Design Configuration and Operational Scenarios for Dynamic Shading Device System

2.2.1. Genetic Algorithms

Since the 1990s, an escalating array of dependable optimization methods, ranging from elementary approaches such as classical calculus to more intricate algorithms like nonlinear programming and evolutionary algorithms, have become accessible to architectural researchers and other professionals. The evolution of optimization algorithms has paralleled advancements in energy analysis software and the proliferation of robust computing technologies, thereby furnishing a diverse spectrum of optimization techniques for the analysis of architectural challenges throughout the design process. Among these techniques, evolutionary algorithms merit particular attention, employing a population of points to sample potential solutions within the solution space and inform the direction of convergence. Noteworthy examples of such algorithms include Genetic Algorithms (GAs) and Particle Swarm Optimization. For this thesis, GAs were deemed more desirable and accessible, given their integration with popular energy analysis software and plugins such as Galapagos or Octopus within Grasshopper for Rhino 7.

From 2013 to 2022, GAs have been widely utilized in the analysis of shading devices, [21]. However, as presented in Table 5, the application of GAs in the case of kinetic shading systems is still limited.

Table 5. Objectives and tools applied in studies on dynamic shading systems (2018–2023).

Cite No.	Objectives	Tools *	Simulation Time
[5]	Presents a practical PDE for the design and fabrication of kinetic architectural elements	R, G, L, Python, and experiment	All working hours/year
[6]	Compare daylighting and visual comfort performance of the two SD types	R, G, D	9:00, 12:00, 15:00 of 21st of Mar, Jun, and Dec
[7]	Investigated the integration process using the normalization method to find an optimal rotational angle of oculi at the given time	R, G, D, Energy Plus	9:00, 12:00, 15:00 of 21st of Mar, Jun, Sep and Dec
[8]	Investigate the possibility of a kinetic system made of vertical aluminum fins	R G, D (Simulation), Arduino (Experiment)	21st of Mar, Jun, Sep, and Dec
[9]	Summarize the coordination process of SMP material programming, design, and fabrication, and analyze the performance of the proposed prototypes	R, G, Cubicreator, and Kangaroo	6:00–18:00 of May 1st and Sep 30th
[10]	Investigate the integration of colored glass from Orosi with interactive kinetic façade triggered by sun timing and occupant’s positions	R, G, D	9:00, 12:00, 15:00 of 21st of Mar, Jun, and Dec

Table 5. Cont.

Cite No.	Objectives	Tools *	Simulation Time
[11]	Identify the best size/rotation angle by fulfilling both LEED V4.1 daylighting requirements and the DA	R, G, D	8:00–16:00 of 21st of Mar, Jun, Sep, and Dec
[12]	Proposes a direction-adjusted kinetic façade design combined with horizontal fins on the south and vertical fins on the west-facing façade	not mentioned	9:00–15:00 of August 14th
[13]	Proposes an SD system to enhance occupants' daylight performance by providing adjustable daylighting strategies through complex forms and movements	R, G, D	9:00, 12:00, 15:00 of 21st of Mar, Jun, and Dec
[14]	A novel method for considering the occupant's position for designing an adaptive façade towards visual and thermal comfort	R, G, H, L	10:00, 13:00, 16:00 of 21st of Mar, Jun, and Dec
[15]	Propose and analyze a louver-type electrochromic façade that can create a uniform indoor illuminance	R, G	9:00 and 15:00 of Mar 20th
[16]	Investigate daylight performance of the expanded-metal shading depicting the sky conditions in Kitakyushu, Japan	R, G, D	12:00 of Dec 21st
[17]	Evaluate the potential energy savings, visual comfort, and economics of the proposed SDs for successful decision-making at the early design stage of retrofitting fully glazed office buildings	Revit-Insight, E-Quest, Dynamo	9:00 and 15:00 of Mar 21st and Sep 22nd
[18]	Investigate suitable façade forms (form-finding) that are effective in providing an appropriate interior environment with natural light using science	R, G, Climate Studio, Wallacei	8:00–18:00
[19]	Investigate the integration of colored glass from Orosi with an interactive kinetic façade triggered by sun timing and the occupant's positions	R, G, H, L, Design Explorer, GMA	9:00, 12:00, 15:00 of 21st of Mar, Jun, and Dec
[20]	Propose an integrated, systematic framework that supports kinetic façades' performance design and decision-making from the projects' early design stages	MOEA, NSGAII, PAES	Not mentioned
[21]	Evaluate EUI and UDI for the best louver configuration scenario for three Canadian cities	R, G, NSGA-II	9:00–17:00
[22]	Find the optimal level of the window area with a squared geometry rotational kinematic model with a horizontal axis in the south façade of an office building in Tehran Model and simulate a responsive façade incorporating Miura-ori techniques to enhance visual comfort for building occupants by considering their location and environmental conditions	R, G, H, L	8:00–16:00 of 21st of Mar, Jun, and Dec
[23]	Utilizes an EnergyPlus-based optimization approach to optimize the specifications and control parameters of smart shading blinds, resulting in significant reductions in building energy consumption, discomfort glare index (DGI), and predicted percentage of dissatisfied occupants (PPD)	R, G, H, Energy Plus, D, BCMO	9:00, 12:00, 15:00 of 21st of Mar, Jun, and Dec
[26]		R, G, Energy Plus, NSGA-II	Not mentioned

* R: Rhinoceros[®]; G: Grasshopper; D: DIVA; H: Honeybee; L: Lady Bug.

Within this paragraph, apart from elucidating the rationale for selecting the GAs to execute the optimization step for the study, the examination will extend to potential challenges during optimization and the requisite conditions for variables. Initially, the feasibility of optimization studies pertaining to building variables hinges upon both the quantity and nature of variables under consideration. Despite the comprehensive analysis promised by optimization studies, the inclusion of variables in even a rudimentary building model can exponentially escalate the number of simulation runs, potentially reaching tens of thousands. Notably, the utilization of continuous variables lacking upper thresholds can result in an infinite number of simulations. Optimization techniques furnish a structured decision-making framework guiding the search process within a defined solution space towards a solution that optimally satisfies predetermined criteria, whether maximized or minimized. Particularly pertinent to dynamic shading systems, which adapt to environmental changes over time, variables may encompass climatic factors, temporal conditions, and configuration parameters of shading devices.

Climatic variables, characterized by their unpredictable nature due to the myriad possibilities of real weather contexts, are thus designated as input conditions/assumptions within the scope of this research. Crucially, the temporal variable assumes paramount importance in this study, given its influence on the responsive behaviors of dynamic façades vis-à-vis daylight performance, with sunlight's fluctuating presence throughout daylight hours throughout the year. Consequently, the temporal variable significantly impacts

the configuration and operational parameters of shading devices, as dynamic shading systems react to environmental changes hourly through physical actions such as movement, rotation, retraction, or extension. Thus, the geometric properties and operational schemes of shading devices dictate their efficacy in responding to environmental changes. In summary, both climatic variables and configuration variables of shading devices constitute pivotal factors requiring consideration in the optimization process; even with just two sets of these variables, the potential number of genomes and corresponding simulation runs could reach thousands.

GAs typically necessitate greater computational resources and time than many classical optimization techniques when seeking a high degree of accuracy. Considering time-consuming constraints and computational limitations, the optimization procedure was streamlined to ensure adherence to the research timeline while upholding the highest level of accuracy feasible. Consequently, in addition to running the optimization process with the aforementioned two sets of variables, manual or computer-aided double-checks were regularly conducted throughout the research. Furthermore, within Grasshopper, while simulation results from DIVA yield a comprehensive set of daylight metrics, including sDA, ASE, hourly illuminance data, useful daylight illuminance (UDI), daylight autonomy, and continuous autonomy, their computation proves cumbersome and unwieldy for smooth optimization processes. Consequently, optimizing based on DIVA's calculations consistently resulted in errors during execution. Consequently, Honeybee (HB) and Ladybug (LB) emerged as the most suitable alternatives for the prevailing circumstances, as each simulation run by HB and LB consumes less time than DIVA and permits optimization even with prolonged processing times.

The Strength Pareto Evolutionary Algorithm (SPEA), Non-dominated Sorting Genetic Algorithm-II (NSGA-II), and GA (Galapagos) have emerged as the three most prevalent algorithms. NSGA-II and SPEA are oriented towards converging on a set of Pareto-optimal solutions, whereas GA primarily focuses on identifying a singular optimal or near-optimal solution. Consequently, in this study, GA (Galapagos) is employed in the optimization process to examine nearly optimal solutions for both design configurations and operational scenarios of dynamic shading device systems. The optimization methodology, expounded in detail in subsequent paragraphs, encompasses two primary steps: firstly, the methodology for optimizing geometric configurations for shading devices, followed by the exploration of optimal operational scenarios for dynamic shading systems. The simulation methodology is illustrated in the Figure 1.

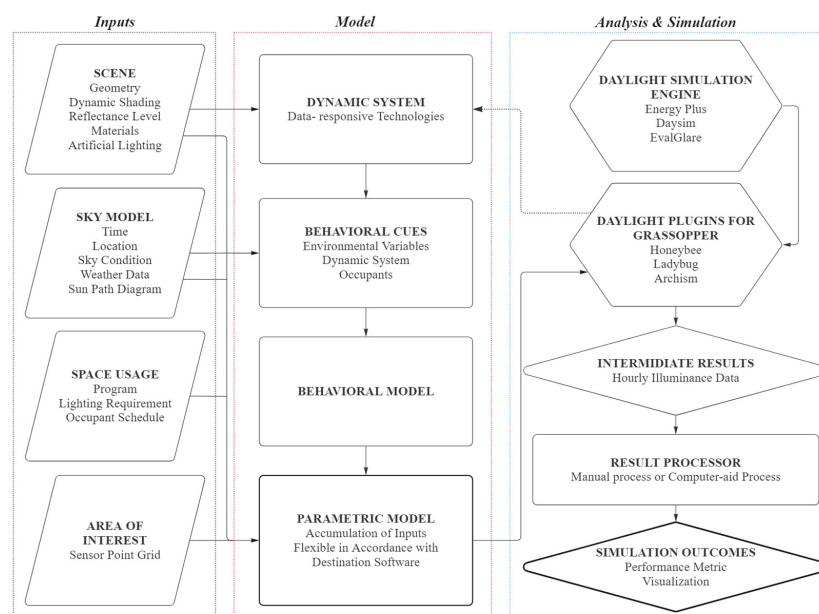


Figure 1. Simulation methods.

2.2.2. Optimization Tool

In recent years, significant advancements have been made in the Grasshopper/Rhino 7 interface with the introduction of its inaugural evolutionary solver, Galapagos, which operates on principles of Evolutionary Computation. Crafted by David Rotten, Galapagos aims to provide a genetic platform for the application of Evolutionary Algorithms across diverse problem domains, catering especially to individuals without programming expertise.

Integral to Galapagos' optimization process is the imperative of clearly defining a problem statement and its corresponding desired outcome. This necessitates the formulation of a fitness function capable of evaluating various solutions with diverse variables. Serving as a yardstick for assessing design products, the fitness function delineates criteria against which solutions are appraised, enabling Galapagos to generate bespoke solutions for the defined problem. These criteria are expressed numerically and fed into Galapagos to guide the optimization process. Through iterative adjustments to these numerical inputs, Galapagos gauges whether the outcomes are converging towards favorable or less desirable conditions, ultimately optimizing design outcomes or resolving defined problems by maximizing or minimizing the fitness function within its feasible numerical range.

Galapagos offers an array of configurable elements within its solver framework, empowering users to manipulate fitness function values. By employing tactics such as "Maximize" or "Minimize," the solver endeavors to maximize or minimize the fitness value, respectively, thereby striving to achieve the highest or lowest possible outcome in accordance with the defined objectives.

2.2.3. Optimization Objectives

The optimization objective, a specific criterion to be maximized or minimized, guides the search process towards defining the optimal solution for a given problem. In this study, the mission is to maximize the daylight performance of dynamic shading devices, evaluated according to the LEED v4.1 daylight requirements scoring system. Spatial Daylight Autonomy (sDA) and Annual Sunlight Exposure (ASE) serve as the key metrics representing these requirements. Thus, the scoring system assesses buildings' daylight efficiency based on the achieved values of sDA and ASE. While maximizing sDA and minimizing ASE simultaneously appears ideal, concerns raised by Christoph Reinhart [27] highlight the challenge of balancing these metrics, particularly with the stringent ASE threshold potentially compromising the quality of illuminated spaces. Therefore, it is essential to evaluate the situation and potential possibilities before seeking the optimum solution. Consequently, the adjusted optimization target aims to maximize sDA and minimize ASE as much as possible, aligning with standard requirements, which mandate 55% floor area for sDA and 10% floor area for ASE. However, flexibility is necessary depending on how dynamic shading devices manage sunlight and solar radiation.

Traditional simulations using DIVA or HB&LB are inadequate for calculating proper values of sDA and ASE for movable shading systems due to the lack of specific algorithms. Elghazi, Y., Wagdy, A. and Abdalwahab, S. [28] proposed two new hourly daylight metrics, Hourly Spatial Daylight Autonomy (HsDA) and Hourly Sunlight Exposure (HSE), as alternative indicators for achieving sDA and ASE targets. These metrics, based on illuminance values at each sensor point hourly, offer a viable approach. Achieving sDA and ASE targets becomes feasible if HsDA approaches the maximum value and HSE reaches the minimum value. In summary, optimization objectives are attainable by maximizing the percentage of floor area exceeding 300 lx and minimizing the percentage exceeding 1000 lx.

2.2.4. The Methodology for Optimizing the Design Configuration for Dynamic Shading Panels

The methodology for optimizing the design configuration for dynamic shading panels consists of the following steps:

1. Perform an optimization with "Month" and "n" variables. The value of "Month" ranges from 1 to 12, corresponding to January to December, respectively. The shift in the sun's direction's vector during the change in "Month" causes the shading panel

- tilt angle to transition. The best solution from this optimization will result in the best optimization objective for all months.
- Conduct another optimization to search for the best shading configuration to meet the optimization objective at every time step within a month. This optimization utilizes up to three variables: "Date", "Hour", and "n". The "Date" value ranges from 1 to 31, corresponding to the 1st day to the 31st day of each month, respectively. The variable "Hour" includes values corresponding to all occupied hours of a day, from 8:00 am to 6:00 pm. Changes in both the "Date" and "Hour" variables, like the "Month" variable, affect the opening angle of each panel in response to solar radiation.
 - Visualize the best solutions from the two optimization processes on an excellent graphic to identify their relationship. The variable "n" is common to both optimization processes, while the outcomes derived from each optimization will be the optimum variables of each method. Therefore, if the two optimization processes result in a similar value of "n," that value will be considered the best solution for both operations and can meet all requirements. Suppose no typical result emerges from the two processes. In that case, it can be concluded that the shading device cannot achieve the best optimization objective in any scenario or with any modification of the design configuration.

2.2.5. Methodology of Optimizing Operational Scenarios for Dynamic Shading Device System

The comparative study seeks to identify the optimal operational scheme for shading device systems, focusing on the impact of shading panels on indoor daylight adequacy. The study emphasizes the importance of the rotation angle in achieving desired performance. To determine the optimum operational scenario, 90 simulations are conducted for each occupied hour of the year, covering rotation angles from 0 to 90 or 180 degrees, depending on the type of movement. For each day, 900 simulations are run to cover the ten occupied hours, and this process is repeated every day of the year. The results are scored based on optimization objectives, providing detailed guidance on the ideal rotation angles for each hour of each day. This operational scheme enables shading panels to react hourly to environmental changes, ensuring the best daylight performance and meeting optimization conditions.

3. Results

3.1. Compare Daylight Performance of Dynamic Shading Device System with Static Façades

It is evident from Figures 2 and 3 that dynamic shading systems are more effective in regulating daylight for indoor spaces than static cases.

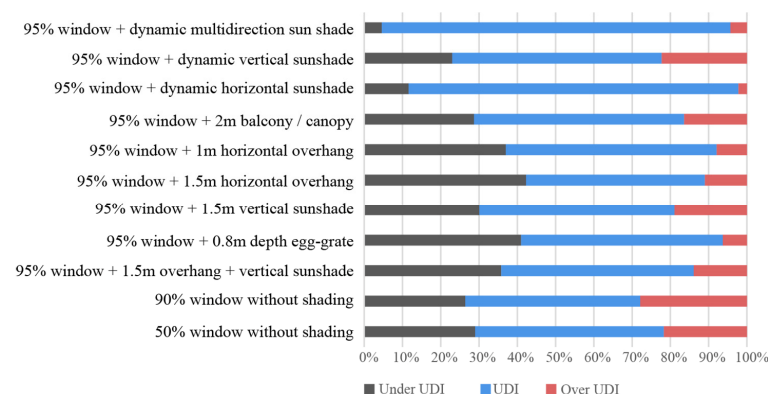


Figure 2. A comparison of UDI values between different cases of dynamic and static façades.

The dynamic multi-directional and horizontal shading systems perform much better than dynamic vertical ones in providing beneficial daylight and reducing the percentage of under-lit and over-lit spaces. Moreover, dynamic shading systems have the potential to reduce the ASE and thereby help reduce the risk of glare, which is a significant factor in ensuring occupant comfort and well-being. However, it is worth noting that although the

dynamic shading systems in the study exceed the standard threshold of 10% for ASE, they still perform better than static cases. Overall, the analysis provides a reliable methodology for assessing the impact of dynamic shading systems on daylight performance and can serve as a helpful tool for designing energy-efficient buildings.

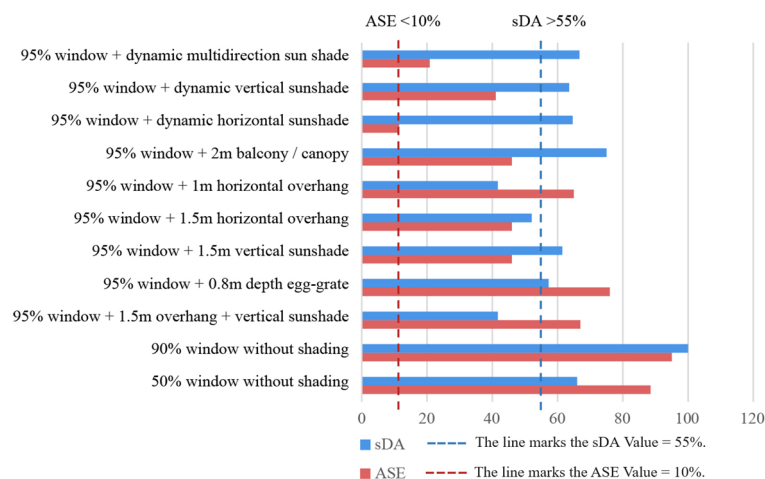


Figure 3. A comparison of sDA and ASE metrics between different cases of dynamic and static façades.

3.2. Compare Daylight Performance between Variations in Dynamic Shading Device Systems

Different shading panels and size variants of each type were assigned as case studies (Table 6 and Appendix A—Figure A1). These typologies would have experimented with simulating and daylight metric calculation to analyze their performance in enhancing daylight.

Table 6. Case studies of dynamic shading device systems.

Case Study	Shading Device System
Case A1	95% window + Vertical dynamic sunshade (n2)
Case A2	95% window + Vertical dynamic sunshade (n4)
Case A3	95% window + Vertical dynamic sunshade (n5)
Case A4	95% window + Vertical dynamic sunshade (n8)
Case A5	95% window + Vertical dynamic sunshade (n16)
Case B1	95% window + Horizontal dynamic sunshade (n2)
Case B2	95% window + Horizontal dynamic sunshade (n4)
Case B3	95% window + Horizontal dynamic sunshade (n5)
Case B4	95% window + Horizontal dynamic sunshade (n8)
Case B5	95% window + Horizontal dynamic sunshade (n16)
Case C1	95% window + Multi-directional dynamic sunshade (n2)
Case C2	95% window + Multi-directional dynamic sunshade (n4)
Case C3	95% window + Multi-directional dynamic sunshade (n5)
Case C4	95% window + Multi-directional dynamic sunshade (n8)
Case C5	95% window + Multi-directional dynamic sunshade (n16)

The following graphs illustrate the comparison of UDI, sDA and ASE metrics for each case. Figure 4 shows that the size of the shading panels significantly impacts their ability to provide adequate daylight in the case studies.

In particular, the under UDI values are dramatically affected by the panel sizes, especially in cases A and B. For case A, the under UDI metric is inversely related to the over UDI metric and the variation “n”. A dimensional sunshade significantly increases the under UDI values while only slightly decreasing the over UDI values. It can be observed that the under-UDI values and the over-UDI values produced by case A are higher compared to cases B and C. The UDI value is favorable for case B and its variants. Although there is a slight deviation in the under UDI values, overall, they reach the smallest values compared

to other cases. In other words, they are unaffected by “*n*” and permanently maintained at an ideal threshold. Surprisingly, there is a significant difference in the value of metrics when the size of case C decreases from 800 mm to 250 mm (from *n* = 5 to *n* = 16). As the UDI values decrease, the under-UDI and the over-UDI values increase considerably.

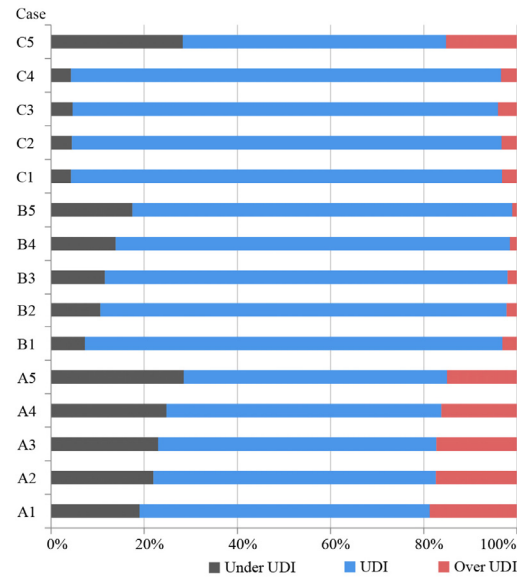


Figure 4. A comparison of useful daylight illuminance values between the case studies.

While UDI is a helpful metric for evaluating daylighting performance, more information is needed to provide a complete picture of how well a shading system works. To obtain a more comprehensive view, we must consider two other metrics: sDA and ASE. As mentioned earlier, ASE is essential for identifying potential issues with glare. Figure 5 illustrates that the vertical shading system allows too much direct sunlight into the indoor space, resulting in ASE values much higher than the LEED v4.1 threshold of 10%. However, reducing the size of the shading panels can significantly decrease the ASE values, although they may still exceed the threshold. In contrast, the horizontal shading system can effortlessly achieve excellent ASE values.

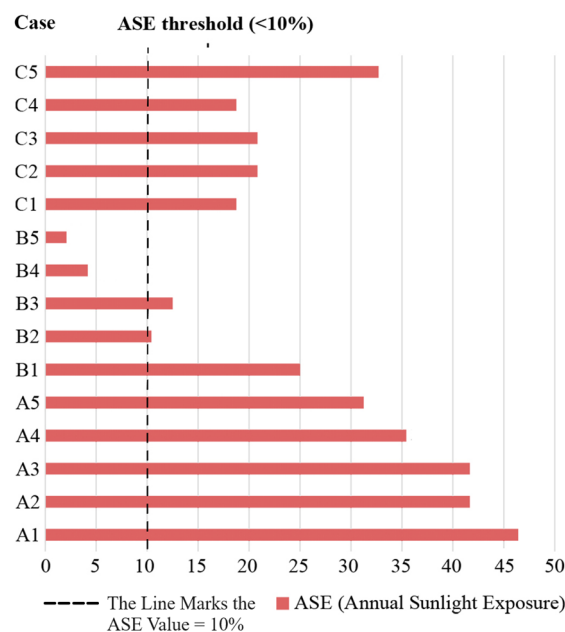


Figure 5. A comparison of ASE metric between the case studies.

The sDA metric is also crucial for assessing daylight performance, as it measures the percentage of occupied hours in which a minimum illuminance level is met. Figure 6 indicates that most shading variants perform well according to sDA requirements, except for a few cases where the shading panel size is tiny.

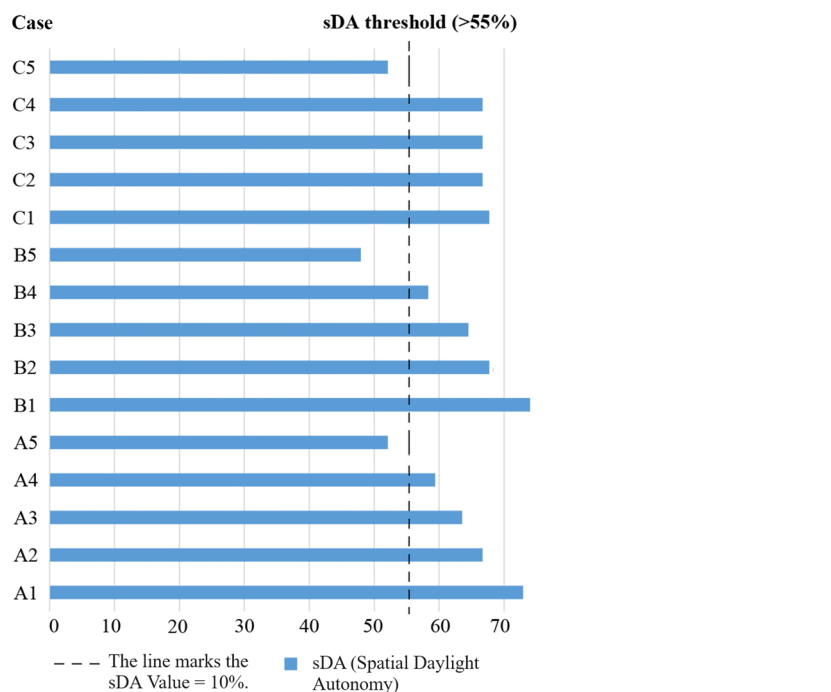


Figure 6. A comparison of the sDA metric between the case studies.

In conclusion, the findings of this section offer a comprehensive comprehension of the efficacy of diverse, dynamic shading panels, which will aid in elucidating the subsequent analysis of the investigation. Based on daylight metric calculations, the horizontal dynamic shading apparatus was identified as having more benefits than the other two systems. The multi-directional dynamic shading panel confers stability in daylighting; conversely, the vertical system's efficiency needs to be improved.

3.3. Influences of Shading Device Configuration on Daylight Performance

3.3.1. Geometric Configuration

Figures 7–9 display the average illuminance values for each occupied hour on the 21st day of each month. These figures serve as examples in Figures A2–A4, illustrating illuminance data by hours and months for each case. The illuminance values generally reach their maximum at noon and gradually decrease in the morning and evening. Daylight in space comprises direct and indirect light, which can be categorized according to their illuminance magnitudes. Illuminance values greater than 1000 lx are classified as direct sunlight, which can cause “glare” conditions.

As demonstrated in Figure 7, the vertical shading panel enables more direct sunlight to enter the indoor space than other shading systems due to its geometrical characteristics. Since direct sunlight is the primary daylight source in indoor areas, reducing illuminance values directly corresponds to decreased daylight. Notably, during winter, when the sun is positioned lower in the sky than in summer, direct sunlight can penetrate deeper into the room. As a result, vertical shading systems are more suitable for colder climate zones where direct sunlight can reduce energy consumption for heating during winter. In summary, the results from illuminance measurements under the influence of dynamic vertical shading systems with varying sizes of shading panels indicated no significant differences in daylighting efficiency between cases. This finding suggests that identifying an optimal geometric configuration for a vertical shading system is unlikely.

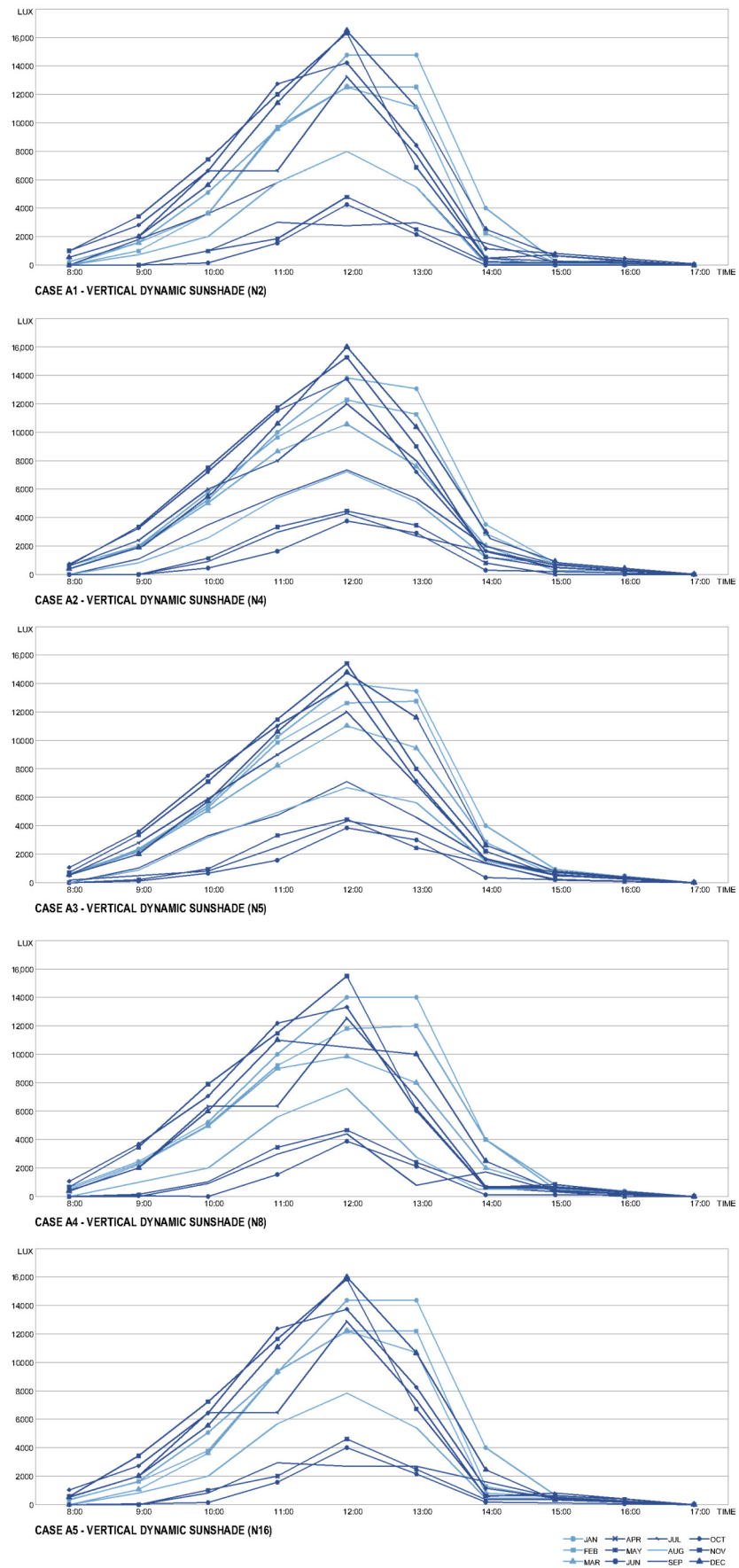


Figure 7. A comparison of daylight performance between variations in vertical shading panels.

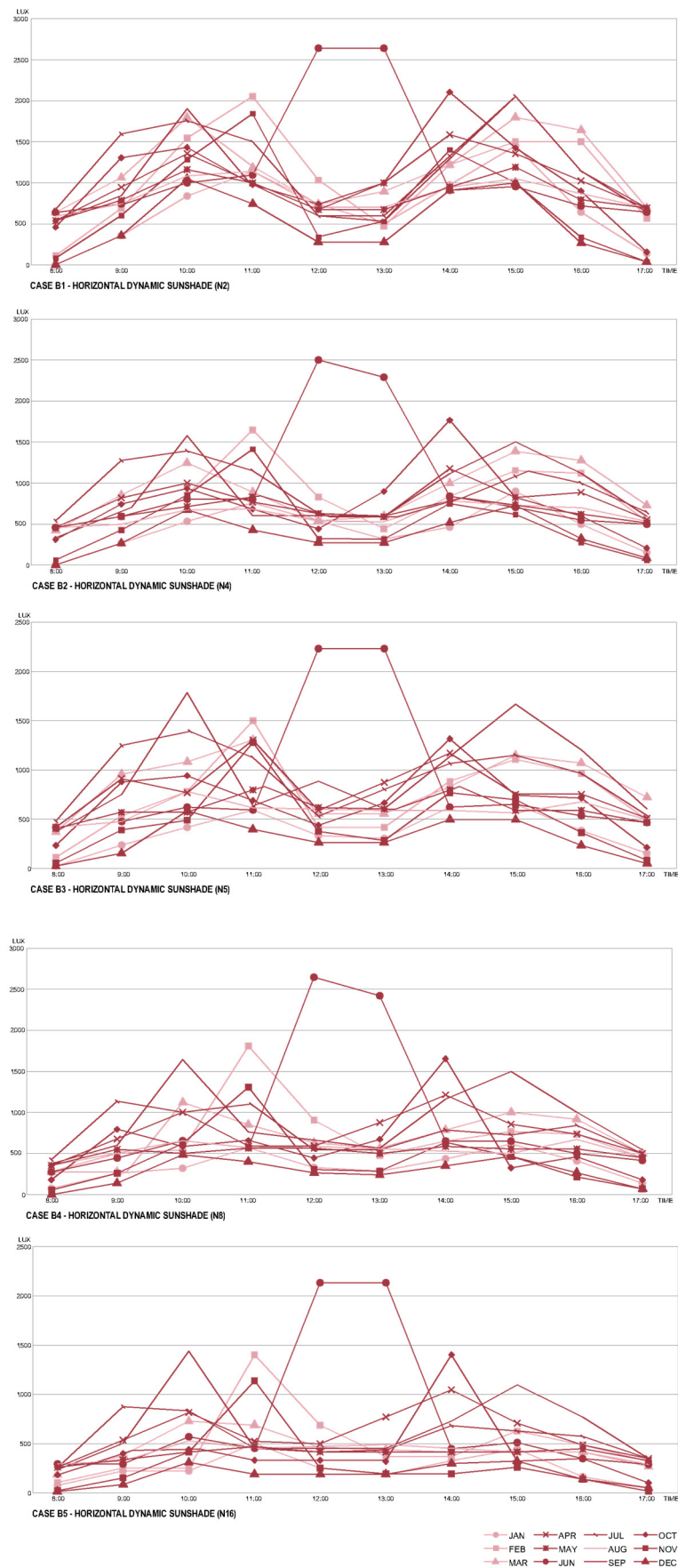


Figure 8. A comparison of daylight performance between variations in horizontal shading panels.

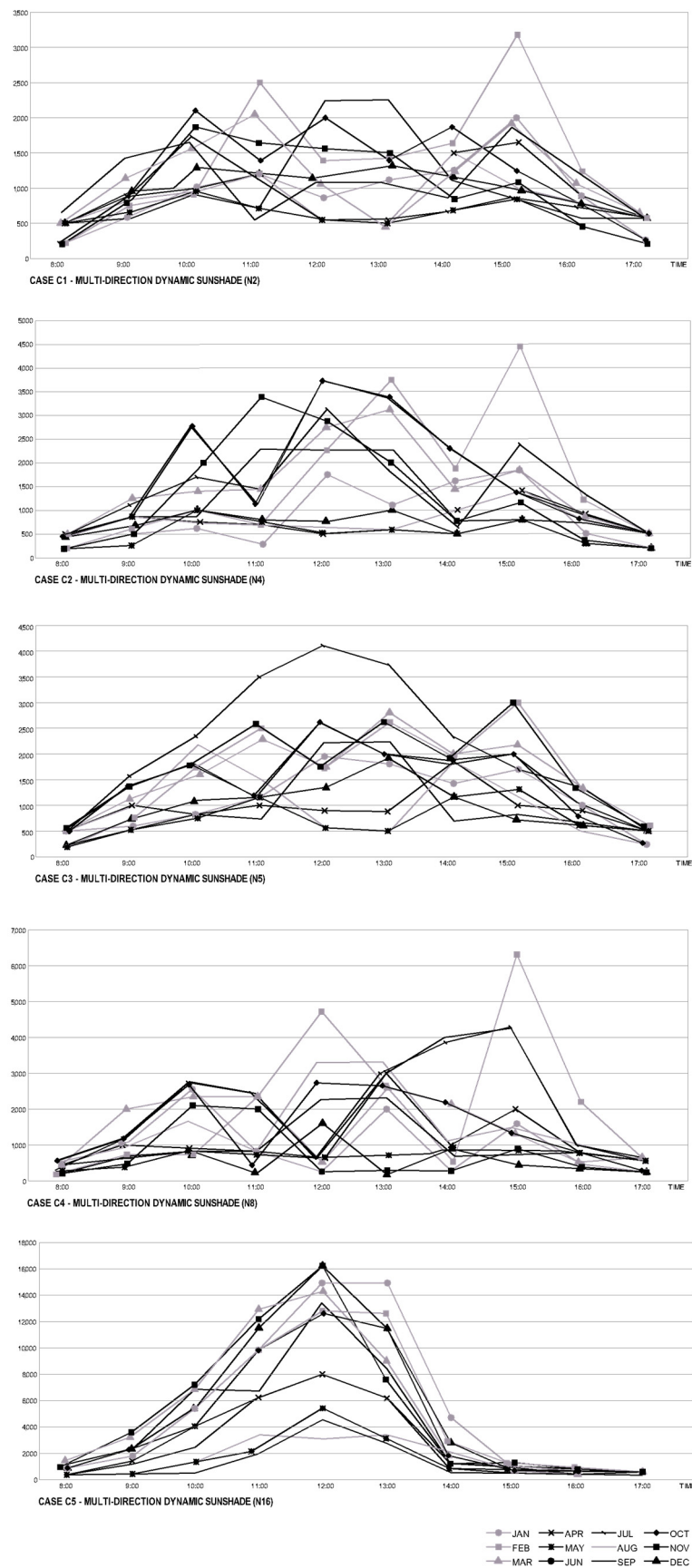


Figure 9. Comparison of daylight performance between variations in multi-directional shading panels.

A glance at Figure 8 shows that the horizontal sunshade system displays a more consistent variability in illuminance values than the other two shading systems. Across months, except for June, the illuminance values range from 300 lx to 2000 lx, which is considered an ideal range for UDI estimation. However, during the last month of winter and early spring, the illuminance values could be much higher and barely reach an acceptable threshold. The hourly illuminance value chart for case $n = 2$ (the most extensive shading panel) indicates that the highest values range from 1000 lx to 2000 lx monthly. Furthermore, by decreasing the size of the shading panel from 2 m to 500 mm, the risk of “glare” was reduced by 50%. Ultimately, it is worth noting that the horizontal shading panel system has significant potential for achieving an optimal configuration that enhances daylight performance.

The multi-directional sunshade type utilized in this study consists of simple shading devices with vertical and horizontal shapes exhibiting straightforward motions. Consequently, the findings cannot be generalized to all scenarios and may expose specific weaknesses in regulating daylight. Nevertheless, within the confines of this investigation, the shading panel’s motion characteristics are hypothesized to significantly impact the dynamic façade system’s daylight performance. Therefore, a prototype with a configuration that satisfies the fundamental research objectives was selected to reduce analysis complexity.

Figure 9 shows that the illuminance values of multi-directional shading panels exhibit significant hourly variability, a characteristic of this type of sunshade. Additionally, the values change drastically when resizing the panels. The charts demonstrate that the shading panel’s dimension is inversely proportional to the stability and magnitude of illuminance values. For instance, the most giant shading device ($n = 2$) attains a peak of approximately 3000 lx. However, when the size is reduced to 250 mm ($n = 16$), the maximum values surge to 16,000 lx. Consequently, smaller dimensions enhance daylight uniformity, enabling more direct sunlight to penetrate indoors. As the size decreases, the number of surfaces for reflecting reduces. In other words, a large multi-directional shading panel results in a “blocking” characteristic, while a small commission facilitates “penetration” for the façade system.

3.3.2. Rotation Angle of the Shading Panel

In this study, various experiments were conducted with different rotation angles of the shading panel to investigate their impact on daylight performance. When aligned, the rotation angle α is the angle between the sun’s direction vector and the normal vector of the panel’s surface. The experiments were carried out with variations in α , which is α plus 15 degrees, α plus 30 degrees and with a constant value of $\alpha = 45^\circ$ (that means rotation angle will be static and unchangeable) as listed in Table 7.

Table 7. The case studies of the rotation angle (tilt angle) of the shading panel.

Case	Rotation Angle
A	α
B	$\alpha + 15^\circ$
C	$\alpha + 30^\circ$
D	$\alpha = 45^\circ$

The findings from the experiments suggest that the daylight performance of indoor space is significantly affected by changes in the rotation angle α , particularly for the horizontal and multi-directional shading panel systems. The illuminance values for the horizontal system show no significant difference between cases A and B, but a dramatic increase is observed for case C. In the case of the multi-directional system, changes in rotation angle resulted in a significant difference in illuminance values compared to the original ones. The case with α plus 15 degrees is suggested as the best choice for this type of shading panel. These findings demonstrate the potential to search for an optimal configuration and operating scheme for horizontal and multi-directional shading panel systems.

3.4. Outcomes from Optimization Processes

After conducting an analysis in the previous section and running several optimization tests, it was determined that the vertical shading device could not achieve an optimal configuration for improved daylight performance. Consequently, optimization efforts will be directed toward only two types of sunshades, horizontal and multi-directional, to search for an optimal solution.

3.4.1. Optimizing Geometric Configuration for Horizontal Shading Device

“Genome” is generated by genes that serve as optimization variables. Initially, “Month” and “ n ” are assigned as the optimization variables. The optimization objective is represented by the “objective” values, which assess and score genomes, with a higher value indicating greater satisfaction with the result. Figure 10 illustrates that the maximum value of “objective” is 11.88, corresponding to the 701st genome created by variable $n = 6.7$, with a size of 0.6 m. Based on this, it can be concluded that the optimal size for the horizontal shading device is 0.6 m, resulting in improved daylight performance throughout the year.

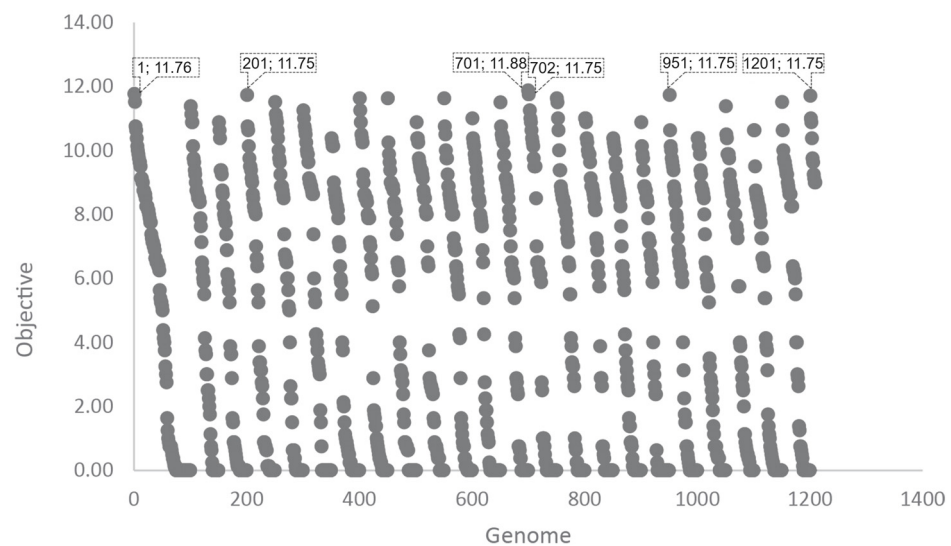


Figure 10. Clusters of optimization results of the horizontal shading system by months.

In the next step, the study process will involve executing the optimization process with variables “day” and “ n ” for each month. Below is an example of the optimization process for March.

Figure 11 depicts the total number of genomes generated, which is approximately 700. Meanwhile, Figure 12 illustrates the best solution with March’s highest optimization objective value. The results reveal that the optimal value for the variable “ n ” is 6, consistent with the value obtained from the optimization process for all months. Similar procedures are applied to analyze the data and interpret the graphs for the remaining months, and the results indicate that the values of “ n ” range from 6.5 to 7.5. The next step involves comparing the results to manually search for the most typical value or range of common values.

Figure 13 displays the correlation between the variable “month”, “ n ”, and optimization objectives. During this phase, all other variables except for “ n ” are treated as input conditions for the process. Based on the graph, it can be inferred that the values of “ n ” fall within the range of 6.6–6.7, which corresponds to a 0.6 m width of the horizontal shading panel.

The same methodology was utilized to determine the optimal geometric configuration for the multi-directional shading device. Figure 14 illustrates that the optimal solutions for each month have one common optimal variable, which is 9. This value corresponds to a 0.45 m (444 mm) dimension of the panel’s vertical and horizontal sides. By using this size of shading device, the dynamic façade can achieve improved daylight performance.

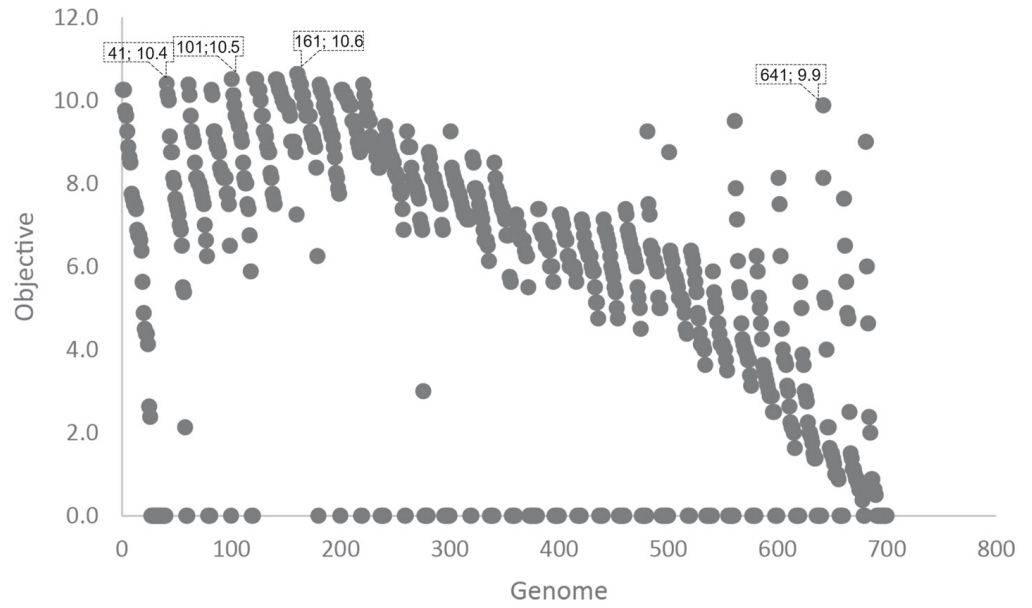


Figure 11. Clusters of optimization results of the horizontal shading system in March.

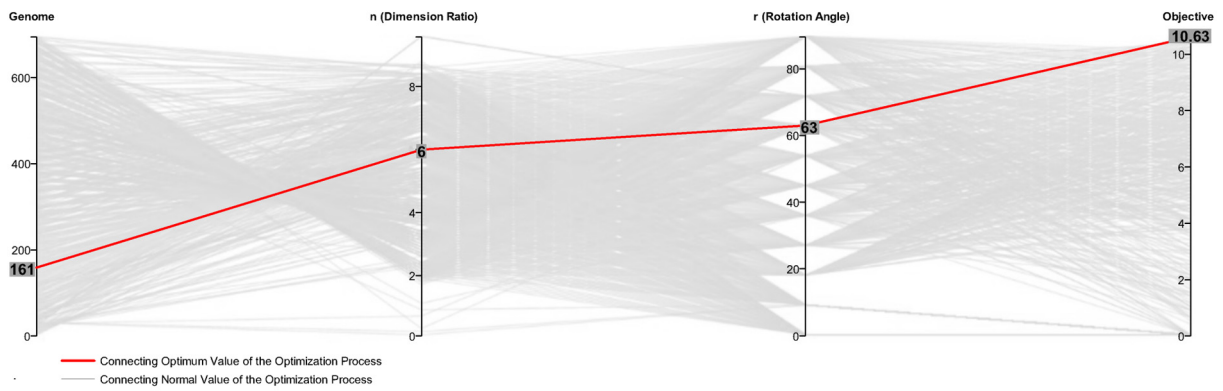


Figure 12. The relationship between the number of genomes, values of variables and optimization objectives of the horizontal shading system in March.

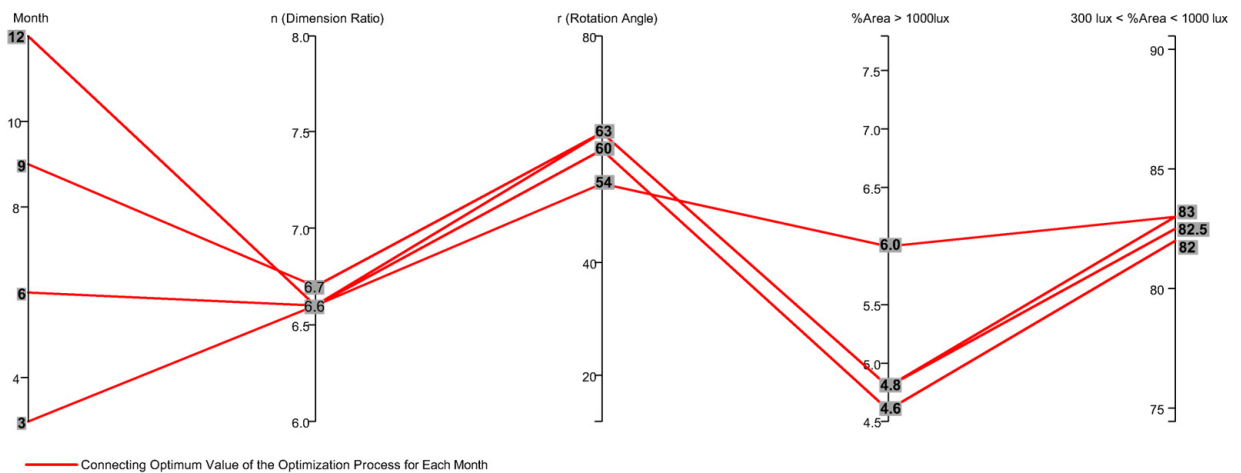


Figure 13. A comparison of the optimal solution of each optimization process of the horizontal shading system for each month.

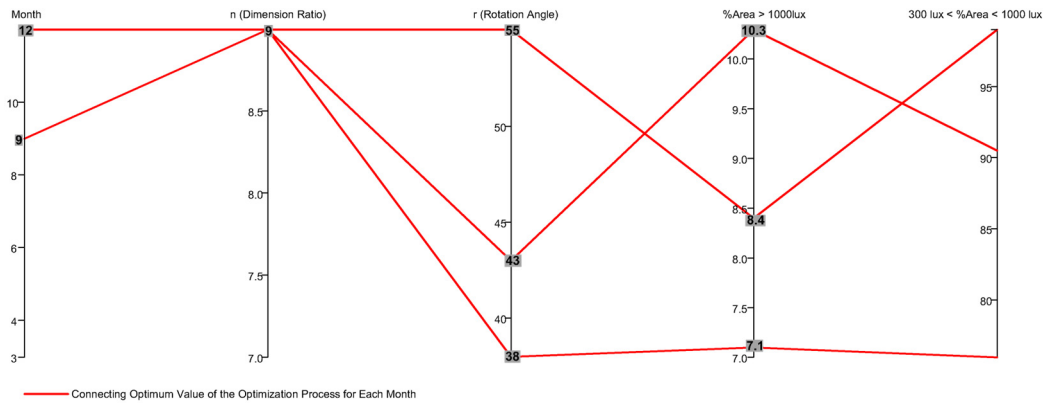


Figure 14. A comparison of the optimal solution of each optimization process of the multi-direction shading system for each month.

3.4.2. Optimizing an Operational Scenario for Dynamic Shading Device System

After determining the optimal size of the panels, the next step involves identifying the optimal rotation angle for every occupied hour of the day. To accomplish this, hourly simulations were conducted for each rotation angle value to evaluate all possible scenarios and determine the best solution. The selection and assessment processes are performed manually by comparing the optimization objectives, which include Hourly Spatial Daylight Autonomy (HsDA) and Hourly Sunlight Exposure (HSE).

An example of the results of this process is presented in Figure 15. The table comprises the horizontal axis indicating the hours in a day and the vertical axis representing the rotation angle ranging from 0 to 90 degrees. To interpret the results, for every hour, the shading panel will have 90 potential movements corresponding to 90 different rotation angles. Each angle generates an optimal value of the optimization objective hourly. By identifying the most desirable value, an optimal rotation angle range can be determined, which is depicted by the blue-colored zone.

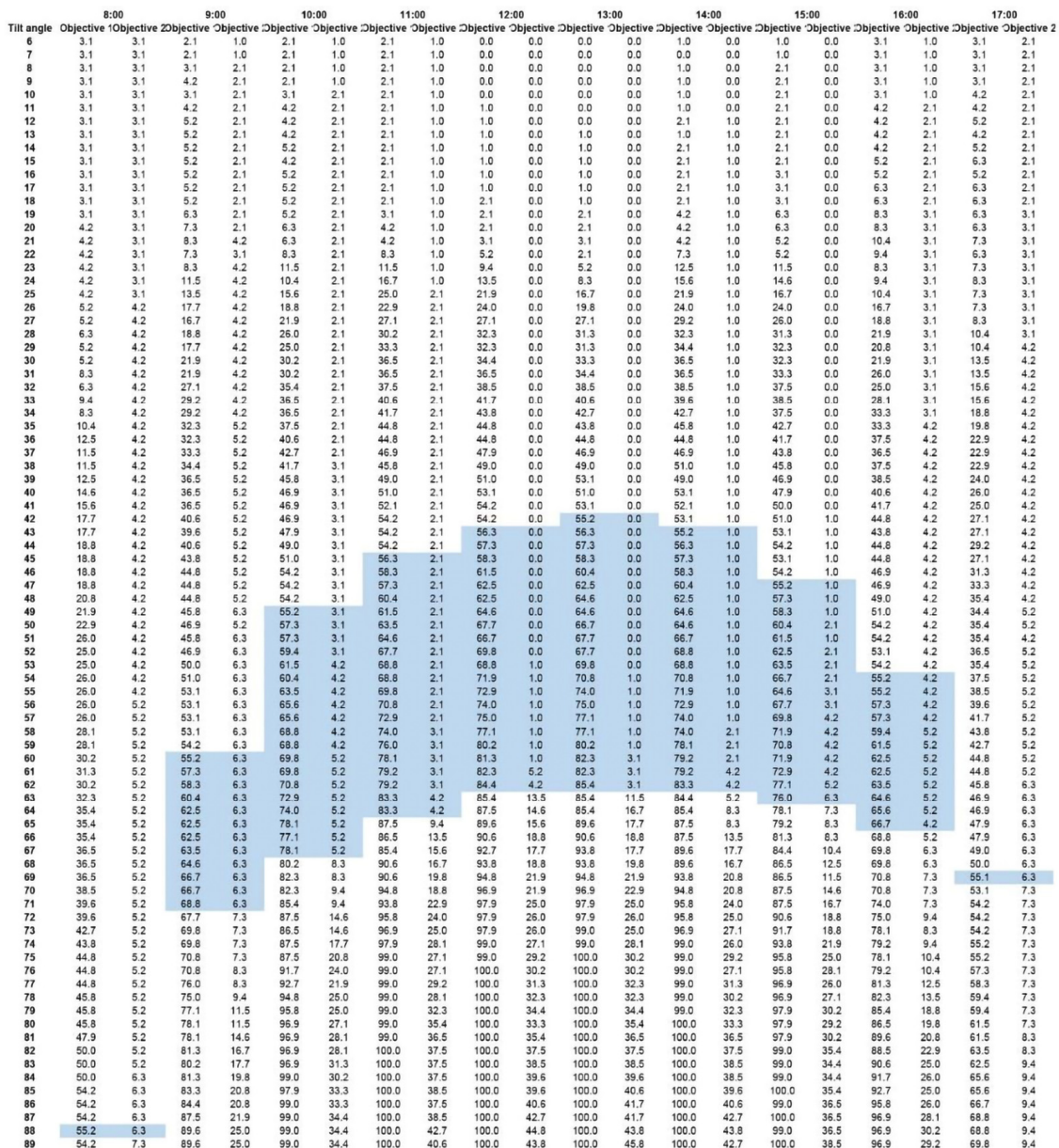
The optimal rotation angles for each occupied hour of the horizontal and multi-directional shading devices on the 21st day of March, June, September, and December are shown in Tables 8 and 9.

Table 8. Table of the optimal rotation angles for each occupied hour of the horizontal shading device (21st day of March, June, September, and December).

Months \ Hours	Hours									
	8:00	9:00	10:00	11:00	12:00	13:00	14:00	15:00	16:00	17:00
Mar 21st	88°	60–71°	49–67°	45–64°	43–62°	43–62°	43–62°	47–63°	54–65°	69°
Jun 21st	60–71°	69–89°	55–89°	50–89°	46–72°	46–74°	48–89°	54–89°	66–89°	76°
Sep 21st	78–89°	56–74°, 48–49°, 56°, 63°	48–68°	44–63°	42–63°	42–63°	44–63°	48–68°	59–69°	84–89°
Dec 21st	65–66°	48–49°, 56°, 63°	47–57°	46–55°	44–54°	44–54°	45–56°	46–60°	48°, 60°	64–67°

Table 9. Table of the optimal rotation angles for each occupied hour of the multi-directional shading device (21st day of March, June, September, and December).

Months \ Hours	Hours									
	8:00	9:00	10:00	11:00	12:00	13:00	14:00	15:00	16:00	17:00
Mar 21st	71–85°	48–53°	42–46°	33–34°	39–40°	32°; 38°	34°	43°	43–44°	59–64°
Jun 21st	70–89°	64–83°	53–65°	45–54°	43–45°	43°	45–53°	49°; 50–64°	61–79°	66°; 67–89°
Sep 21st	62–89°	41°; 46–47°	42°	34°	36°	40°	39–40°	42–43°	44°	65–72°; 73°
Dec 21st	45–68°	36–41°	36–37°	33°; 37°	35°	34°	34–35°	35–36°	38°	66°



which satisfies the research objectives, was selected as a prototype for the experiment. Despite the study's limitations regarding factors considered and assumptions made, the findings demonstrate that optimizing the configuration and operating scheme of dynamic shading panels can significantly enhance the quality of indoor daylighting.

This study contributes significantly by introducing a high-precision methodology for hourly daylight simulations and proposing methods to optimize dynamic shading panels. Dynamic shading systems present challenges due to their unpredictable and flexible movements in response to environmental stimuli. As kinetic façade motion occurs over time, any analysis of dynamic systems must be conducted hourly, resulting in hundreds of thousands of simulations running. Furthermore, the outcomes of these processes are raw data, such as illumination data, which require additional programming tools, such as Python and Fortran, to process and calculate. Although these methods provide highly accurate findings, they are time-consuming and have a high computational interruption risk.

This study aims to determine the most effective geometric configuration and operational scenario for a dynamic shading device system to improve daylight performance on a selected date of the year. Before searching for an optimal solution, experiments were conducted to examine the potential for successful optimization for each shading panel type. These experiments assessed the impact of shading panel configuration on daylight performance for different geometrical types, sizes, and rotation angles. Notably, while adjustments to shading device configuration resulted in significant changes in the daylight performance of horizontal and multi-directional shading panel types, the impact on vertical shading device type was minimal. This indicates that horizontal and multi-directional types have a higher potential for achieving optimal configurations for better daylight performance. The search results confirmed this hypothesis, revealing an optimal dimension of approximately 0.6 m for the horizontal shading device type and 0.45 m for the multi-directional shading device type. Furthermore, optimal operational scenarios were proposed, including sets of the optimum rotation angles for each type.

4.1. Limitations

The domain of dynamic shading devices and kinetic façades exhibits a diverse array of characteristics not comprehensively discussed in the preceding chapters. However, constraints pertaining to time and computational infrastructure necessitated a focused examination solely within the realm of daylighting, with assessments confined to the locale of Icheon City. Despite initial intentions to encompass various locations with disparate climatic profiles, the study's scope was constrained by practical considerations.

This research endeavors to discern the daylight performance disparities among different types of shading panels. While numerous variations exist within the multi-directional type beyond the basic horizontal and vertical panels, the complexity inherent in addressing all permutations was deemed impractical. Consequently, a simplified prototype of the multi-directional shading panel, aligning with research objectives and computational feasibility, was selected to streamline analysis.

As previously delineated, certain analyses were temporally constrained to mitigate research duration. However, such limitations did not compromise the accuracy of results, as they did not significantly impact critical evaluations such as Spatial Daylight Autonomy (sDA) or Annual Sunlight Exposure (ASE) calculations.

Moreover, the study encountered challenges stemming from the time-intensive nature of data simulation and processing, exacerbated by unforeseen computer interruptions.

4.2. Future Research Opportunities

The temporal constraints inherent in this study are emblematic of the methodological challenges encountered, particularly in managing vast datasets. Leveraging programming tools such as Python and Fortran proved instrumental in surmounting these challenges, underscoring their indispensable role in thesis completion. Notably, Python's user-friendly interface facilitated the development of building energy performance analysis tools like

Honeybee or Ladybug. This underscores the potential for developing novel digital tools tailored to dynamic architectural systems.

While this study primarily addresses issues related to daylight performance, future research should broaden its scope to encompass additional facets of building energy efficiency, including energy consumption and maintenance costs associated with dynamic shading systems.

Furthermore, acknowledging the vast array of dynamic shading panel types beyond those examined herein, future investigations should strive to encompass a more comprehensive range of variations. Such endeavors promise to enrich the design framework for kinetic façades, building upon the insights gleaned from this research.

One notable contribution of this study lies in elucidating the limitations inherent in different types of dynamic shading devices. Subsequent studies could delve into strategies for mitigating these limitations, particularly concerning vertical shading device systems.

Author Contributions: Conceptualization, methodology, validation, supervision, D.-H.K.; software, formal analysis, visualization, H.T.L.; data curation, writing—original draft preparation, H.T.L. and T.T.N.; writing—review and editing, T.T.N. All authors have read and agreed to the published version of the manuscript.

Funding: This work was supported by the National Research Foundation of Korea (NRF) grant funded by the Korea government, (MSIT) (grant number 2023R1A2C1007170).

Data Availability Statement: The raw data supporting the conclusions of this article will be made available by the authors on request.

Conflicts of Interest: The authors declare no conflicts of interest.

Appendix A

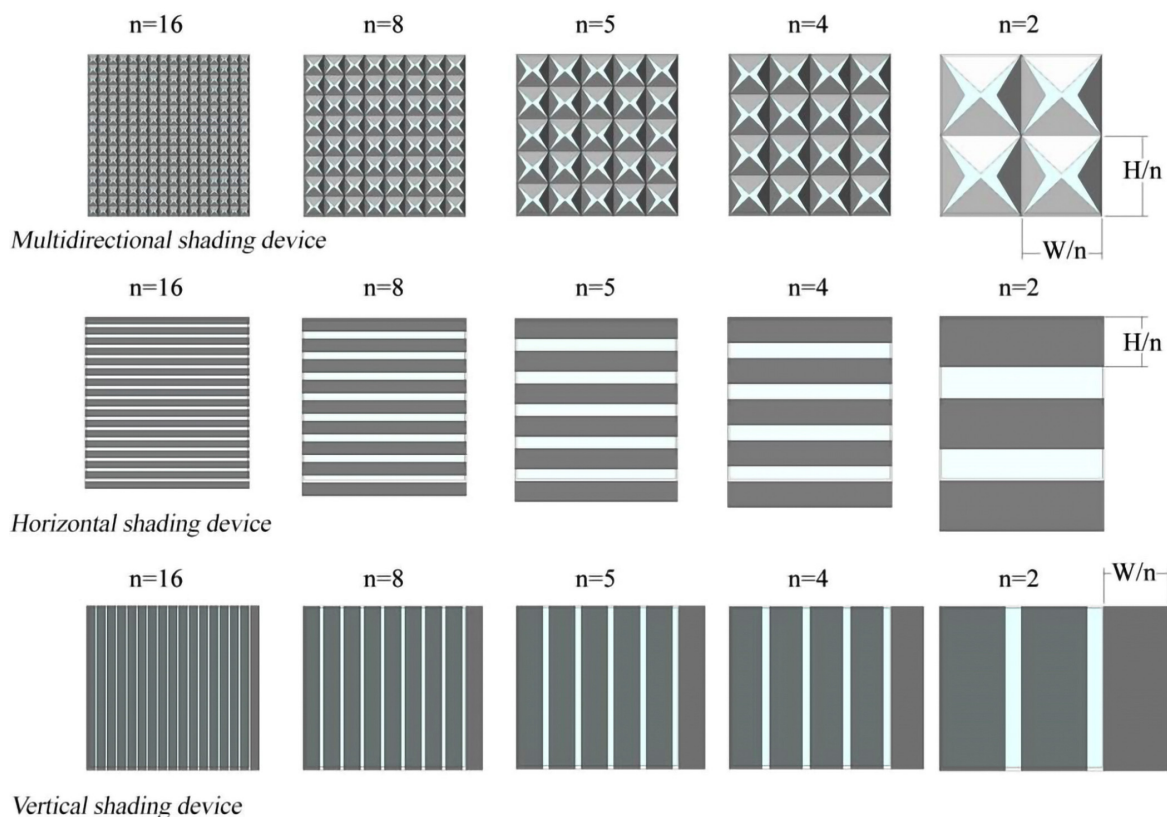


Figure A1. The case studies.

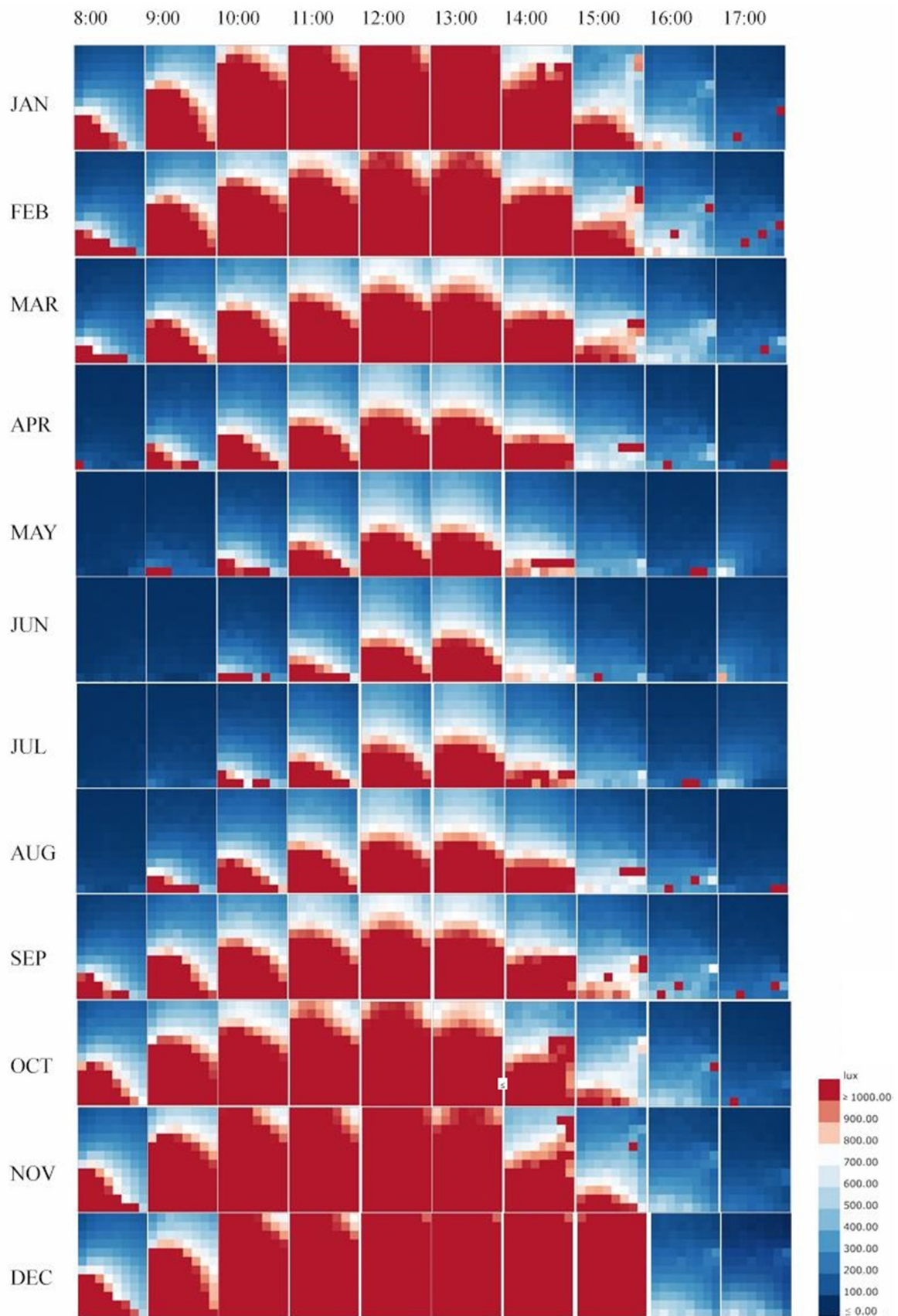


Figure A2. Illuminance data by hours and months of case A3—vertical dynamic shading devices (n5).

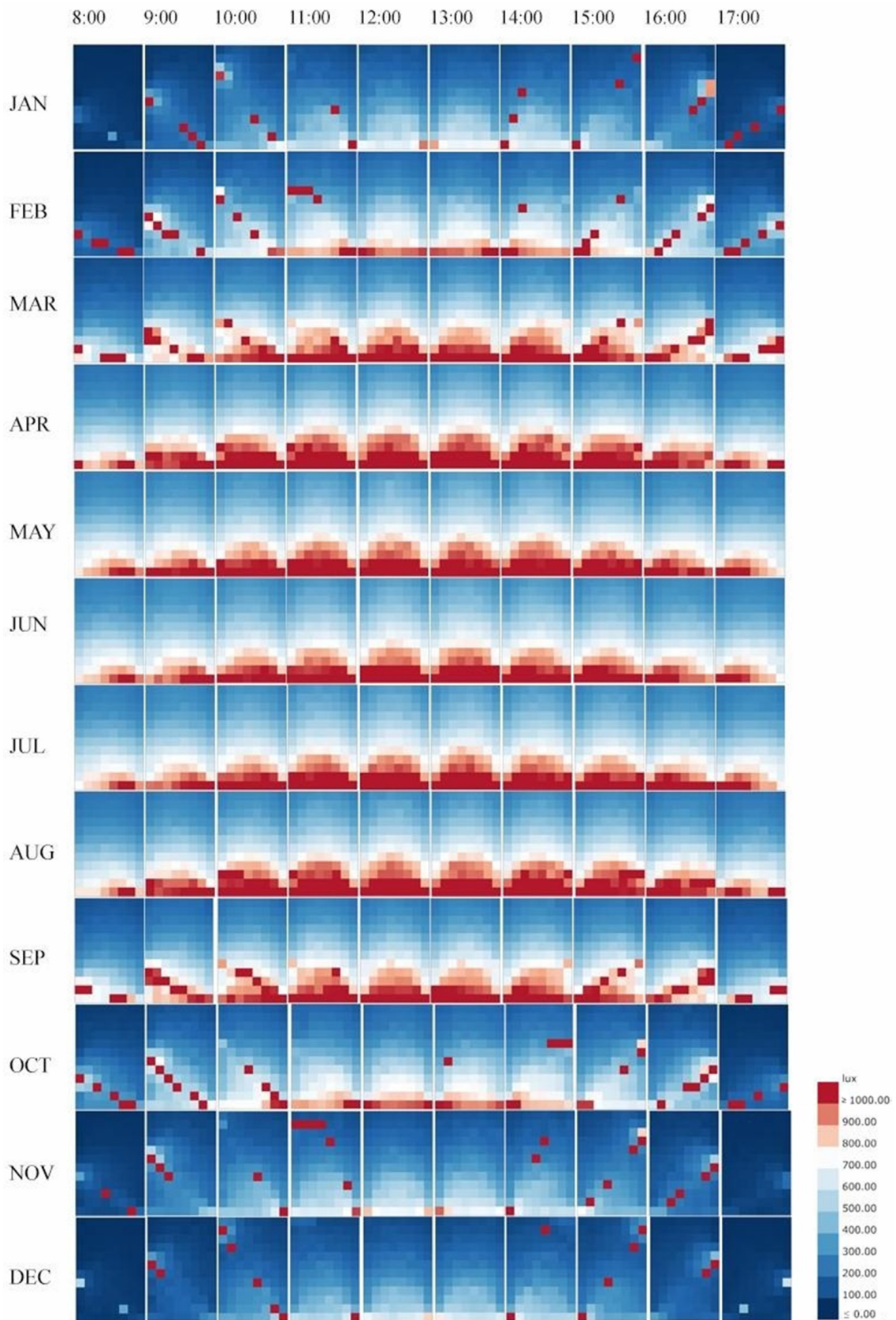


Figure A3. Illuminance data by hours and months of case B3—horizontal dynamic shading devices (n5).

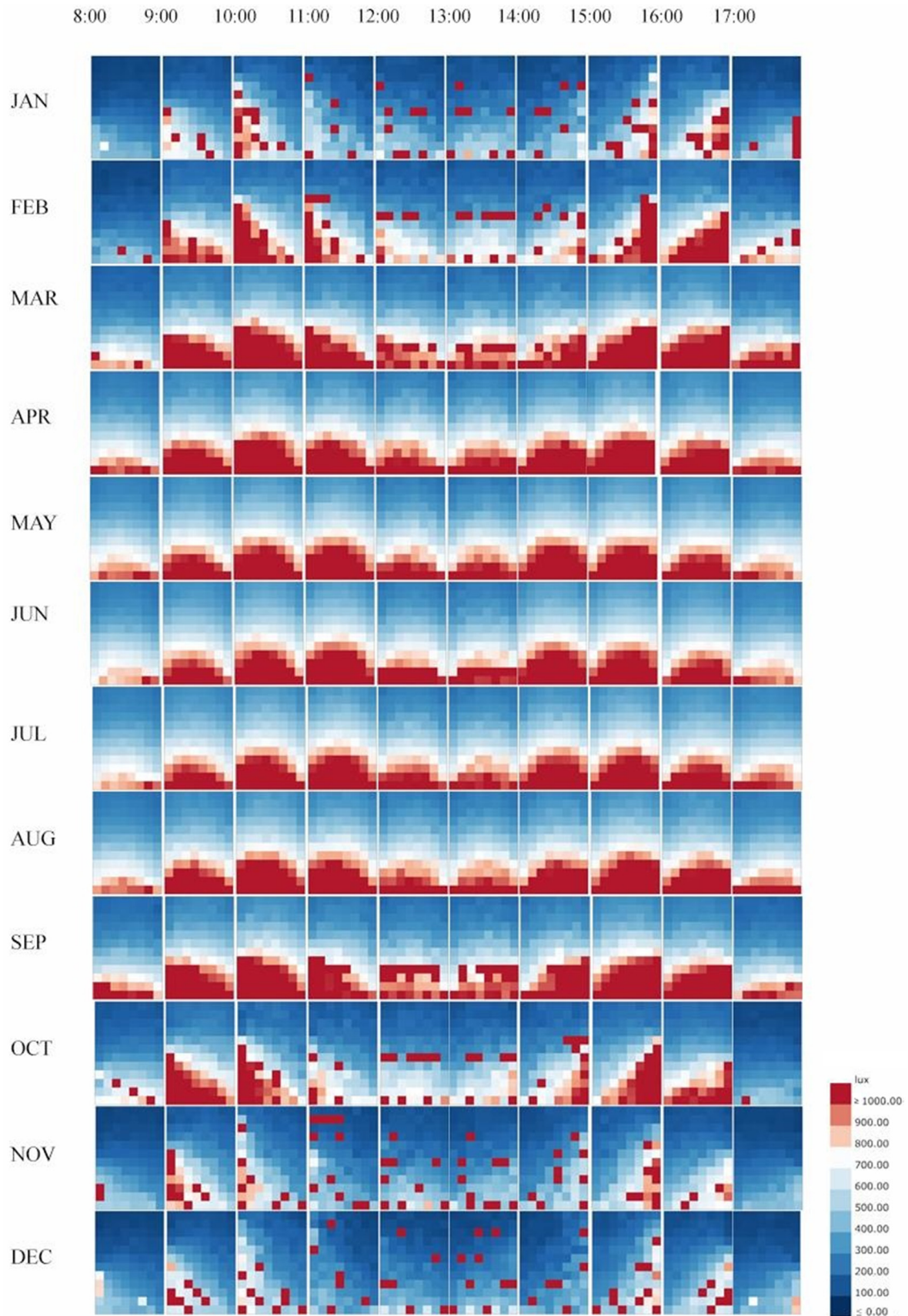


Figure A4. Illuminance data by hours and months of case C3—multi-directional dynamic shading devices (n5).

References

1. Zuk, W.; Clark, R.H. *Kinetic Architecture*; Van Nostrand Reinhold: Washington, DC, USA, 1970.
2. Moloney, J. *A Framework for the Design of Kinetic Façades. Computer-Aided Architectural Design Futures (CAAD Futures) 2007*; Springer: Dordrecht, The Netherlands, 2007; pp. 461–474. [[CrossRef](#)]
3. Al-Masrani, S.M.; Al-Obaidi, K.M.; Zalin, N.A.; Isma, M.I.A. Design optimisation of solar shading systems for tropical office buildings: Challenges and future trends. *Solar Energy* **2018**, *170*, 849–872. [[CrossRef](#)]
4. Tabadkani, A.; Roetzal, A.; Li, H.X.; Tsangrassoulis, A. Design approaches and typologies of adaptive façades: A review. *Autom. Constr.* **2021**, *121*, 103450. [[CrossRef](#)]
5. Jayathissa, P.; Caranovic, S.; Hofer, J.; Nagy, Z.; Schlueter, A. Performative design environment for kinetic photovoltaic architecture. *Autom. Constr.* **2018**, *93*, 339–347. [[CrossRef](#)]
6. Hosseini, S.M.; Mohammadi, M.; Guerra-Santin, O. Interactive kinetic façade: Improving visual comfort based on dynamic daylight and occupant's positions by 2D and 3D shape changes. *Build. Environ.* **2019**, *165*, 106396. [[CrossRef](#)]
7. Im, O.-K.; Kim, K.-H.; Amirazar, A.; Lim, C. A Unified Framework for Optimizing the Performance of a Kinetic Façade. In Proceedings of the Symposium on Simulation for Architecture and Urban Design, Atlanta, GA, USA, 7–9 April 2019; Society for Computer Simulation International: San Diego, CA, USA, 2019; pp. 32–39.
8. Nakapan, W.; Pattanasirimongkol, A. Developing a kinetic façade towards a solar control façade design prototype. In Proceedings of the 4th RSU National and International Research Conference on Science and Technology, Social Sciences, and Humanities 2019 (RSUSSH 2019), Pathumthani, Thailand, 26 April 2019.
9. Yoon, J. SMP Prototype Design and Fabrication for Thermo-responsive Façade Elements. *J. Facade Des. Eng.* **2019**, *7*, 41–62. [[CrossRef](#)]
10. Hosseini, S.M.; Mohammadi, M.; Schröder, T.; Guerra-Santin, O. Integrating interactive kinetic façade design with colored glass to improve daylight performance based on occupants' position. *J. Build. Eng.* **2020**, *31*, 101404. [[CrossRef](#)]
11. Karaseva, L.V.; Cherkhaga, O.A. Conceptual Designs of Kinetic Façade Systems. *IOP Conf. Ser. Mater. Sci. Eng.* **2021**, *1079*, 042053. [[CrossRef](#)]
12. Hosseini, S.M.; Fadli, F.; Mohammadi, M. Biomimetic Kinetic Shading Façade Inspired by Tree Morphology for Improving Occupant's Daylight Performance. *J. Daylighting* **2021**, *8*, 65–85. [[CrossRef](#)]
13. Kim, J.-H.; Han, S.-H. Indoor Daylight Performances of Optimized Transmittances with Electrochromic-Applied Kinetic Louvers. *Buildings* **2022**, *12*, 263. [[CrossRef](#)]
14. Khidmat, R.P.; Fukuda, H.; Kustiani Paramita, B.; Qingsong, M.; Hariyadi, A. Investigation into the daylight performance of expanded-metal shading through parametric design and multi-objective optimisation in Japan. *J. Build. Eng.* **2022**, *51*, 104241. [[CrossRef](#)]
15. Chandrasekaran, C.; Sasidhar, K.; Madhumathi, A. Energy-efficient retrofitting with exterior shading device in hot and humid climate—Case studies from fully glazed multi-storied office buildings in Chennai, India. *J. Asian Archit. Build. Eng.* **2022**, *22*, 2209–2223. [[CrossRef](#)]
16. Sankaewthong, S.; Horanont, T.; Miyata, K.; Karnjana, J.; Busayarat, C.; Xie, H. Using a Biomimicry Approach in the Design of a Kinetic Façade to Regulate the Amount of Daylight Entering a Working Space. *Buildings* **2022**, *12*, 2089. [[CrossRef](#)]
17. Hosseini, S.M.; Heidari, S. General morphological analysis of Orosi windows and morpho butterfly wing's principles for improving occupant's daylight performance through interactive kinetic façade. *J. Build. Eng.* **2022**, *59*, 105027. [[CrossRef](#)]
18. Sadegh, S.O.; Gasparri, E.; Brambilla, A.; Globa, A. Kinetic façades: An evolutionary-based performance evaluation framework. *J. Build. Eng.* **2022**, *53*, 104408. [[CrossRef](#)]
19. Sanakaewthong, S.; Miyata, K.; Horanont, T.; Xie, H.; Karnjana, J. Kinetic Façade Design with Eshelby Twist for Sunlight Exposure Reduction. In Proceedings of the 2022 International Conference on Cyberworlds (CW), Kanazawa, Japan, 27–29 September 2022; pp. 8–15. [[CrossRef](#)]
20. Sangtarash, F.; Fayaz, R.; Nikghadam, N.; Matini, M.R. Optimal window area of a kinetic facade to provide daylight in an office building in Tehran. *Space Ontol. Int. J.* **2022**, *11*, 61–75. [[CrossRef](#)]
21. Rafati, N.; Hazbei, M.; Eicker, U. Louver configuration comparison in three Canadian cities utilizing NSGA-II. *Build. Environ.* **2023**, *229*, 109939. [[CrossRef](#)]
22. Kahramanoğlu, B.; Çakıcı Alp, N. Enhancing visual comfort with Miura-ori-based responsive facade model. *J. Build. Eng.* **2023**, *69*, 106241. [[CrossRef](#)]
23. Choi, H.S. Kinetic Photovoltaic Façade System Based on a Parametric Design for Application in Signal Box Buildings in Switzerland. *Appl. Sci.* **2023**, *13*, 4633. [[CrossRef](#)]
24. Reinhart, C.F. *Daylighting Handbook. II, Daylight Simulations, Dynamic Facades*; Stein, R., Ed.; Building Technology Press: Cambridge, MA, USA, 2018.
25. Field, K.; Deru, M.; Studer, D. Using DOE Commercial Reference Buildings for Simulation Studies. In *SimBuild 2010*; National Renewable Energy Laboratory: New York, NY, USA, 2010. Available online: <https://www.osti.gov/servlets/purl/988604> (accessed on 4 May 2023).
26. Naderi, E.; Sajadi, B.; Behabadi, M.A.A.; Naderi, E. Multi-objective simulation-based optimization of controlled blind specifications to reduce energy consumption, and thermal and visual discomfort: Case studies in Iran. *Build. Environ.* **2020**, *169*, 106570. [[CrossRef](#)]

27. Reinhart, C. Opinion: Climate-based daylighting metrics in LEEDv4—A fragile progress. *Light Res.* **2015**, *47*, 388. [[CrossRef](#)]
28. Elghazi, Y.; Wagdy, A.; Abdalwahab, S. Simulation-driven design for the kinetic system; optimise kaledocycle facade configuration for daylighting adequacy in hot arid climates. In Proceedings of the 14th Conference of International Building Performance Simulation Association, Hyderabad, India, 7–9 December 2015; pp. 182–189. [[CrossRef](#)]

Disclaimer/Publisher’s Note: The statements, opinions and data contained in all publications are solely those of the individual author(s) and contributor(s) and not of MDPI and/or the editor(s). MDPI and/or the editor(s) disclaim responsibility for any injury to people or property resulting from any ideas, methods, instructions or products referred to in the content.